J Mol Model (2013) 19:1605–1615
DOI 10.1007/s00894-012-1721-8

ORIGINAL PAPER

Study of DNA base-Li doped SiC nanotubes in aqueous solutions: a computer simulation study

Sepideh Ketabi · Seyed Majid Hashemianzadeh · Morteza MoghimiWaskasi

Received: 19 September 2012 / Accepted: 3 December 2012 / Published online: 3 January 2013

Abstract Due to the importance of soluble nanotubes in biological systems, computational research on DNA base functionalized nanotubes is of interest. This study presents the quantitative results of Monte Carlo simulations of Li-doped silicon carbide nanotubes and its nucleic acid base complexes in water. Each species was first modeled by quantum mechanical calculations and then Monte Carlo simulations were applied to study their properties in aqueous solution. Solvation free energies were computed to indicate the solvation behavior of these compounds. The computations show that solvation free energies of the complexes of DNA bases with Li-doped SiC nanotubes are in the order: thymine > cytosine > adenine > guanine. The results of complexation free energies were also used to study the stability of related structures, which indicate that thymine-Li-doped SiC nanotubes produce the most stable compound among the four DNA base complexes.

Keywords Monte Carlo simulations · Solvation · Free energy perturbation · SiCNT · Li · DNA base

Introduction

Carbon nanotube (CNT) applications have recently become a very important topic especially in the biotechnological sciences, with great potential in areas such as biosensors, and DNA and protein transporters for theraputic purposes [1–7]. From several different aspects of study, the functionalization of CNTs is a very popular topic in contemporary nanotube (NT) literature because the planned modification of CNT properties is believed to pave the way toward real nanotechnology applications [8].

Up to now, the potential of biological applications of CNTs has been rarely explored. The spatial dimensions of NTs are comparable to those of biological ion channels, and they provide a simple model environment in which to understand the primary behavior of water in complex biological systems. Different studies have shown that CNTs have toxic effects on biological systems [9–11]. CNTs were found to elicit pathological changes in the lungs, produce respiratory function impairments, damage the mitochondrial DNA in aorta, increase the percent of aortic plaque, and induce atherosclerotic lesions in the brachiocephalic artery of the heart [12]. However, unlike CNTs, silicon carbide nanotubes (SiCNTs) are not an officially listed hazardous substance.

Recently, it has been found that SiC nanomaterials have less toxic effect than CNTs. Results indicated that, under the experimental conditions used, SiC nanowire in water was not acutely toxic to amphipods [13].

SiCNT is an important material with lots of significant properties. It has a large band gap, possesses a reactive exterior surface that facilitates sidewall decoration, and has stability at high temperatures [14, 15]. Therefore SiCNT has many applications in electronic devices operating under harsh conditions of high temperature, power, and frequency [16].

Another problem affecting use CNTs in biological systems is their poor solubility in physiological solutions. In contrast to the hydrophobic surface of CNTs, the SiC surface is hydrophilic [17]. The existence of a specific charge arrangement in SiCNTs makes them attractive alternative materials for solution phase. Therefore it seems that SiCNT are better candidates for application in biological systems because of their higher solubility [18].

S. Ketabi (✉)
Department of Chemistry, East Tehran Branch, Islamic Azad University, Tehran, Iran
e-mail: sketabi@qdiau.ac.ir

S. M. Hashemianzadeh · M. MoghimiWaskasi
Molecular Simulation Research Laboratory, Departments of Chemistry, Iran University of Science and Technology (IUST), Tehran, Iran

According to the literature, a 50 % SiCNT is the best suggested structure in this category of mixed nanotubes [19, 20]. Theoretical studies [19, 21–24] performed on the structure and stability of SiCNTs have shown that the most stable structures contain Si and C atoms at a ratio of 1:1, and nanotubes with only Si–C bonds have higher binding energies than those containing Si–Si and C–C bonds in addition to Si–C bonds. In fact, among energetically stable forms of SiCNTs, the one in which the Si and C atoms have alternating positions in the tube wall is full of point charges.

Moreover, an important technique to increase the solubility and reactivity of CNT is through functionalization, which increases the electrical dipole moments and results in enhanced solubility of NTs in water through favorable changes in the free energies of solvation [25]. This property decreases the toxicity of NTs and improves their biocompatibility. Strategic approaches toward increasing the solubility of NTs have been developed mainly through the surface functionalization of either covalent or non-covalent attachments to the sidewalls of NTs [2, 26–31]. Non-covalent functionalization could not only enhance the solubility of NTs but also maintain their attractive geometric, electronic and mechanical properties. Among numerous functional species for solubilizing NTs, biological and bioactive materials have special importance. Functionalization of NTs with the assistance of biological molecules improves the solubility of NTs in aqueous or organic environments, thus facilitating the application of NTs in biotechnology, biomedicine, and bioengineering. Nucleic acids (DNA and RNA) have been explored in terms of non-covalent functionalization of NTs in various biomedical applications ranging from nanodevices, gene therapy and drug delivery to membrane separation [32–34]. Non-covalent interactions and the ability of nucleobases to disperse CNTs have been investigated both theoretically and experimentally [35–42].

Functionalization using elemental metal can also lead to improved solubility of NTs [43]. Generally, elemental metal-sidewall functionalized nanotubes are soluble in aqueous solvents. As the mostly used alkali metal in these processes, in situ Li has been Raman-studied in detail [44]. The activity of Li in reactions with nucleophiles is higher than that of other alkali metals due to the larger amount of z/r for Li. Theoretical study of the interactions between isolated DNA bases and various group IA metal ions [45] indicated that interaction energies for DNA base–Li complexes are larger than with other alkali metals. In fact, an increase in the atomic number or z/r ratio leads to a decrease in interaction energy. In addition, the weight of Li doped NTs is less than with other alkali metals. Thus, we use Li-doped NT for enhancement of activity in aqueous solutions.

Attachment of known coordinating ligands such as nucleic acid bases to the surface of NTs via suitable metals like Li may modify the chemical and physical properties of NTs. DNA bases have the ability to coordinate to a variety of metals. This property could be used for the stabilization of superstructures as well as to support metal-aided catalytic transformations. Therefore, new hybrid materials comprising both nucleobases and NTs would be extremely interesting in view of the remarkable properties of NTs and recognition properties of nucleobases. Consequently, an investigation into (1) the coordination of nucleic acid bases with metal doped NTs, and (2) the stability and solubility of these compounds were the purposes of this study.

The solvation energies of Li-doped SiCNT(SiCNT-Li) and its complexes with purine and pyrimidine DNA bases were studied in order to evaluate the effect of complexation of DNA bases with metal-doped nanotubes on solvation. Monte Carlo simulation and perturbation methods were used to calculate solvation free energies and compare solubility of these compounds. In addition, complexation free energies of adenine (A), guanine (G), cytosine (C) and thymine (T) with SiCNT-Li were computed to compare the stability of these structures. Our results provide fundamental knowledge of new biological compounds of more soluble SiCNT in water and pave the way for more experimental explorations of new nanomaterials in bionanotechnology.

Computational details

The interaction between the solute and the solvent molecules plays an essential role in the various molecular processes involved in chemistry and biochemistry. In this study, the solvation of complexes of SiCNT-Li with DNA base in the presence of water was studied in order to understand the interaction between H_2O molecules and these complexes. The research comprised two sections: quantum mechanics and Monte Carlo simulation. In the quantum mechanical part, isolated molecules were optimized. The stability of the structures in solution phase was then studied by quantum mechanical calculations. The computed natural atomic charges were used in Monte Carlo simulation in aqueous solutions.

Solvation free energy is the change in Gibbs energy when a molecule is transferred from a vacuum (or the gas phase) to a solvent. In fact, solvation free energy includes two terms: the free energy for taking a nanotube from a pure solid phase into solution, and the free energy for taking a single nanotube out of the solid into the ideal gas state [46, 47]. The solvation energies of nanotubes are inaccessible experimentally due to problems of low volatility. In this case, the application of theoretical methods may be the best approach to gain physical insights into the effects of solvation.

To calculate the solvation free energies of molecules, the thermodynamic perturbation method was applied in these computations. Appropriate steps were taken to obtain the most accurate results possible with a molecular mechanical

based approach; the appropriate force field and the Monte Carlo simulation were used.

Potential energy functions

The computational competence with which the energy can be calculated using a given model is often an important factor as there are a large number of water molecules present, together with a solute. A wide range of force fields have been proposed.

The total potential energy of a chemical system, E_{tot}, includes internal potential energy (E_{int}) and external potential energy (E_{ext}) terms:

$$E_{tot} = E_{int} + E_{ext} \quad (1)$$

The monomers were represented by interaction sites, usually located on nuclei. The interaction energy between two molecules, A and B, were expressed by the pairwise sum of their interaction contributions.

Calculated energy values, as well as various structural parameters, can be used to analyze the solvation energies of nanotubes.

The E_{tot} term can be represented as the sum of the energy contributions from solute–solvent, solvent–solvent, and intermolecular interactions.

Transferable intermolecular potential functions [48, 49] (TIP3) are used for water molecules, and standard Lennard-Jones(LJ) potential to present the short-range potential and long-range Coulombic potential, with parameters ε, σ and q for C and Si in nanotubes [50, 51] and each atom in DNA bases [52, 53] (Table 1). For both models, the pair potential function E_{ij} is represented by Coulombic and Lennard-Jones terms among sites centered on nuclei:

$$E_{ij}^{AB} = 4\varepsilon_{ij}\left[\left(\frac{\sigma_{ij}}{r_{ij}}\right)^{12} - \left(\frac{\sigma_{ij}}{r_{ij}}\right)^{6}\right] + \frac{q_i q_j e^2}{r_{ij}} \quad (2)$$

r_{ij}, q_i, and q_j are the interatomic distance between atoms *i* and *j*, and the atomic charges on atoms *I* and *j*; and ε is well depth of potential . Each type of site has three parameters, a charge in electron, q, ε and σ. The LJ parameters between pairs of different atoms are obtained from the Lorentz–Berthelot combination rules [54].

The TIP3 model uses a total of three sites for electrostatic interactions. The partial positive charges on the hydrogen atoms are balanced exactly by an appropriate negative charge located on the oxygen atom.

Table 1 Lennard-Jones (LJ) parameters for atoms in a solute

Site	ε,kcal mol^{-1}	σ, Å
C	0.08	3.5
Si	0.31	3.804
Li	0.018279	2.12645
O	0.21	2.96
N	0.17	3.25
C in C=O	0.105	3.75
Other C	0.08	3.5
H on N	0	0
H on C	0.05	2.5

Free energy

The free energy difference between two states A and B, of a system may be derived from classical statistical mechanics [55] allowing this difference to be expressed as Eq. 4 as the free energy perturbation (FEP) master equation.

$$\Delta G = G_B - G_A = -RT\ln\langle\exp -(E_B - E_A)/RT\rangle \quad (3)$$

$E_E - E_A$ is the potential energy difference between states A and B of the system. *T* is the absolute temperature, and the symbol $\langle\rangle$ indicates an ensemble average.

The solvation free energy of the species A (Li-doped SiCNT and DNA base complexes of Li-doped SiCNT) can be written in terms of perturbations where the species disappear to nothing in the gas phase and in solution:

$$\Delta G_{sol}(A) = \Delta G_{gas}(A \to 0) - \Delta G_{sol}(A \to 0) \quad (4)$$

Absolute free energies of the reaction of DNA base with Li-doped SiCNT were calculated using thermodynamic cycles. Finally, the complexation free energy in solution is given by:

$$\Delta G_r = \Delta G_{sol}(L \to 0) + \Delta G_{sol}(NT \to 0) - \Delta G_{sol}(LNT \to 0) \quad (5)$$

$\Delta G_{sol}(L \to 0), \Delta G_{sol}(NT \to 0)$ and $\Delta G_{sol}(LNT \to 0)$ are solvation free energies of ligand(DNA base), Li-doped SiCNT and DNA base- Li-doped SiCNT complex, respectively.

Geometry optimization

Quantum mechanical calculations were used for isolated solute molecules (DNA bases, SiCNT-Li and SiCNT-Li-DNA base). To avoid dealing with asymmetry effects in the case of non-chiral zigzag structures, the armchair nanotube structures [a (6, 6) SiCNT] were considered as solute samples. DNA bases were coordinated with Li atom in SiCNT-Li. Binding of DNA bases (Fig. 1) and SiCNT was done via the active sites. Monte Carlo simulation [56], ab initio calculations [45] and also experimental data [57] have indicated that most binding sites of DNA bases were observed to be N_7 in adenine, and N_7 and with minor binding at O_6 in guanine. The amino group in adenine and guanine is not involved in

coordination, because its lone pair participates in the ring π system. So, bonding of a metal-doped nanotube to adenine and guanine occurs at N_7. The most favorable site for binding in cytosine is the N_3site in the aqueous or gas phase. N1 and N3 in thymine are the most active sites towards metal. These sites have lone pairs available for participating in coordination. Therefore, these sites of DNA bases are seen to interact with SiCNT-Li. Each species (SiCNT-Li, SiCNT-Li-A, SiCNT-Li- G, SiCNT-Li-C, and SiCNT-Li-T) was optimized by the DFT/B3LYP method using the 6–31 G*[58] basis set. In all calculations, nanotubes were capped with hydrogen atoms. Natural bond orbital (NBO) theory was applied to optimized geometries to determine natural atomic charges.

The calculations were performed by using the GAMESS-US quantum chemistry package [59]. The optimized structures of four SiCNT-Li-DNA base compounds are shown in Fig. 1. In the subsequent simulation step, these geometries were applied. Since uncapped NTs were used in the simulation section, hydrogen atoms are not shown in Fig. 2.

Carbon and silicon around Li in SiCNT-Li species is indicated in Fig. 3. The natural atomic charges of carbon and silicon atoms near the Li have been included in Table 2. In subsequent calculations, quantum mechanical charges have been used.

Monte Carlo simulations

Monte Carlo simulations are carried out in a standard manner using Metropolis sampling technique [60] in canonical (T, V, N) ensemble at 300 K.

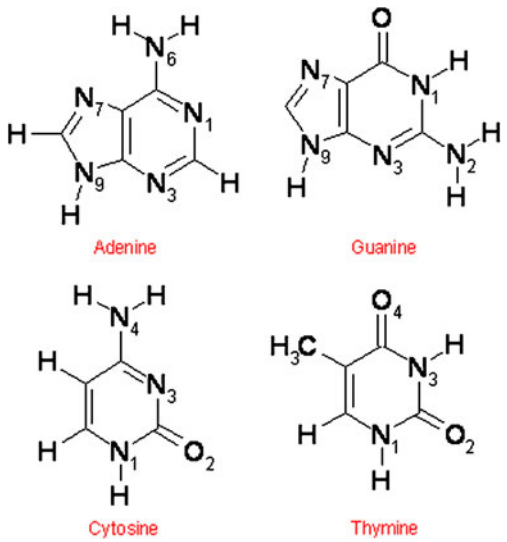

Fig. 1 DNA bases

Each setup included two fragments: a solute fragment and water molecules. Solute fragments were SiCNT-Li; adenine, guanine, cytosine and thymine and their complexes with SiCNT- Li.

All calculations were performed in a cubic box at the experimental density of water, 1 g cm^{-3}. The edges of the box are 50×50×50 Å, which corresponds to almost 4,000 H_2O molecules of pure solvent. The symmetry center of the solutes is in the geometrical center of the cell. A spherical cut off for the potential at an oxygen–oxygen separation (distance between oxygen atoms of two water molecules) of half the length of an edge of the cube was used. One molecule was picked and displaced randomly on each move. An acceptance rate of 50 % for new configurations was achieved by using suitable ranges for translations and rotation about a randomly chosen axis.

The energy of a configuration was obtained from the pairwise sum of the dimerization energies for each monomer as usual. In order to find the optimum length of the Markov chains, a series of simulations was conducted. The system was thoroughly equilibrated using 1×10^7 configurations. Every calculation is extended to include as many configurations as are necessary to reduce the statistical error to the level at which calculated energy differences have quantitative significance.

Results and discussion

Total energies

In the Monte Carlo simulations, a very dilute solution of SiCNT-Li and its compounds with adenine, guanine, cytosine and thymine were used. So one molecule of solute has merged in water and the average energies were then calculated from Monte Carlo simulations. As an example, the resultant configuration of the MC simulation of SiCNT–Li–A in water is shown in Fig. 4. This gives a qualitative idea of the formation of the solvation shell around the solute.

The process of solvation of the solute molecule (SiCNTs) in water is:

$$\mathrm{SiCNT(g)} \rightarrow \mathrm{SiCNT(aq)}$$

The total energy of the compounds (including van der Waals and Coulomb interaction) in water was calculated. The average energy (E_{tot}) calculated from Monte Carlo simulations is given in Table 3. This table also includes the number of solvent molecules (N_{H2O}) in the cubic box, STDEV (the standard deviation of the calculated average in the simulation of finite number of steps) and relative errors.

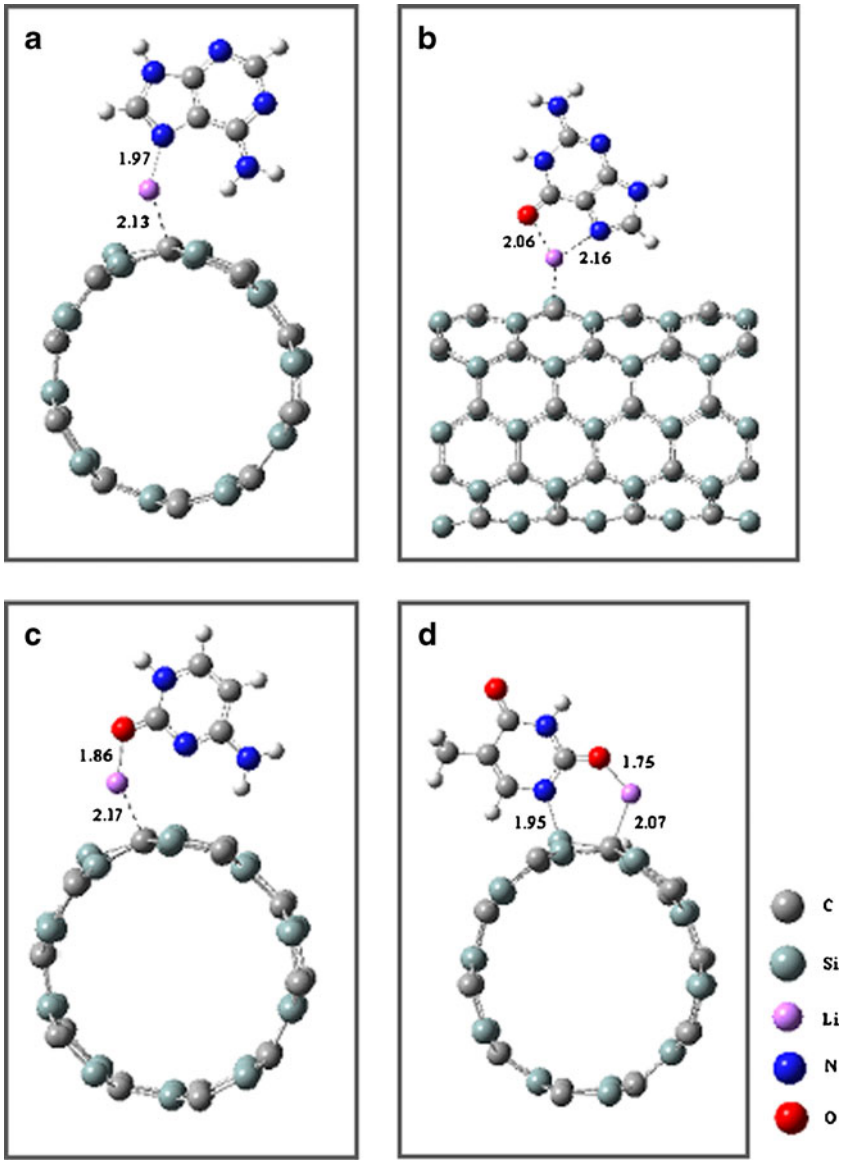

Fig. 2 Optimized structures of DNA base - Li doped Silicon Carbide Nanotubes. **a** SiCNT - Li - A, **b** SiCNT–Li–G, **c** SiCNT–Li–C, **d** SiCNT–Li–T

The results indicate that the absolute solvation energies of these SiCNT compounds in water appear in the following order:

$$E_{total}(SiCNT - Li - T) > E_{total}(SiCNT - Li) > E_{total}(SiCNT - Li - C) > E_{total}(SiCNT - Li - A) > E_{total}(SiCNT - Li - G)$$

In the polar solvent (water), the electrostatic terms play an important role in the solvation energy. Point charges on the material's surface can improve solvation energy because they increase the binding energy of H_2O molecules and the solute. The atomic charges in the solutes affect the electrostatic terms of intermolecular energies directly. As mentioned above, the charges were given from quantum mechanical calculations for all of these NTs. Calculations indicated that the atoms in the nanotube around Li have larger charges when we used thymine (Table 2). In the other ligands (cytosine, guanine and adenine) the charges of carbon and silicon atoms near the Li in nanotube decreased. So, the solvation energies of SiCNT-Li-C, SiCNT-Li-A, SiCNT-Li-G are less than that of SiCNT-Li.

The results are comparable with other experimental and theoretical studies. Quantum mechanical calculations have indicated that thymine more efficiently functionalizes CNT than does cytosine and adenine [61]. This result fundamentally supports the experimental finding that poly T could more efficiently disperse CNTs in water than poly A and poly C [62]. Some theoretical studies have examined the binding of nucleobases with graphene and CNTs [32, 63–65]. The trend of the calculated interaction energies shows some variations. For example, in one of these studies the order of interaction energies of the four nucleobases is: G > T > A > C [63]. These differences are due to intermolecular interactions. Graphene is a carbon allotrope, so it is

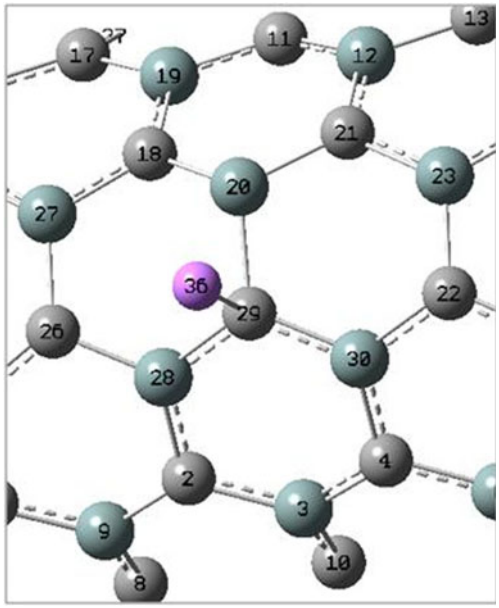

Fig. 3 The site of coordination (Li) and surrounding atoms in SiCNTs

expected that the van der Waals interaction would be the main driving force for the binding between graphene and nucleobases. In recent years, the interaction of nucleobases into silicon nanowire was investigated using a first-principles method based on density functional theory (DFT) [42]. The magnitude of the calculated binding energy shows the following order: G > A ≈ C ≈ T ≈ U.

In fact, in all uncharged NTs, van der Waals interactions make the dominant contribution between the nucleobases and NT. Binding of a DNA base on a charged NT(like SiCNT-Li) is different from the uncharged case. Moreover, in charged NTs, electrostatic interactions make the main contribution between solute and water molecules. In contrast, van der Waals interaction are preferred in uncharged NTs [18].

A simulation can generate an enormous amount of data that should be analyzed properly to extract relevant properties and to check that the calculation has behaved appropriately. One of the factors that determine the accuracy of Monte Carlo calculations is the sample size effect. This factor arises because locating a limit number of molecules in a box followed by subsequent application of periodic boundary conditions introduces error into molecular correlations. For a given system, this effect decreases with the sample size. In most cases of interest, it is not known how to choose the size of the system in order to minimize effect of periodic boundary conditions. The most straightforward test is to perform a series of calculations in which the sample size is systematically increased until the calculated values remain unchanged. The other factor that verifies the precision of Monte Carlo calculations is statistical fluctuations of calculated ensemble averages. Statistical errors are often reported as standard deviations. The errors have been reported in Table 3. As it can be seen in Table 4, the simulation error is under 1 %.

Solvation free energies

The ability to calculate solvation free energies of molecules accurately using thermodynamic perturbation is one of the most important developments in computational chemistry [66]. These methods have wide applicability not only in studies of absolute solvation free energies but also in studies of binding free energies. Although it is important for these

Table 2 Natural atomic charges of atoms near Li in Li-doped silicon carbide nanotube (SiCNT) and its complexes with DNA bases

No. atom	Atom type	Atomic charge				
		SiCLi	SiCLi-A	SiCLi-G	SiCLi-C	SiCLi-T
2	C	−0.96947	−0.96893	−0.96731	−0.98903	−1.93534
3	Si	0.96635	0.96014	0.96412	0.96112	1.92824
4	C	−0.96791	−0.97011	−0.96925	−0.96967	−1.93789
30	Si	0.97429	0.95631	0.97035	0.96631	1.89712
18	C	−0.92401	−0.92821	−0.93304	−0.93069	−1.96194
27	Si	0.96942	0.96539	0.96333	0.96686	1.92869
26	C	−0.98323	−0.95459	−0.95233	−0.95795	−1.91106
28	Si	0.93204	0.9517	0.95911	0.96999	1.87806
30	Si	0.97429	0.95631	0.97035	0.96631	1.89712
22	C	−0.96732	−0.96553	−0.97056	−0.965	−1.93663
23	Si	0.96942	0.96539	0.96333	0.96686	1.92869
21	C	−0.93655	−0.92983	−0.93549	−0.93316	−1.96733
20	Si	1.01062	1.00398	1.03464	1.02747	2.08091
29	C	−0.95703	−0.96663	−0.96048	−0.96992	−2.0626
36	Li	0.42108	0.39257	0.36838	0.39673	0.83614

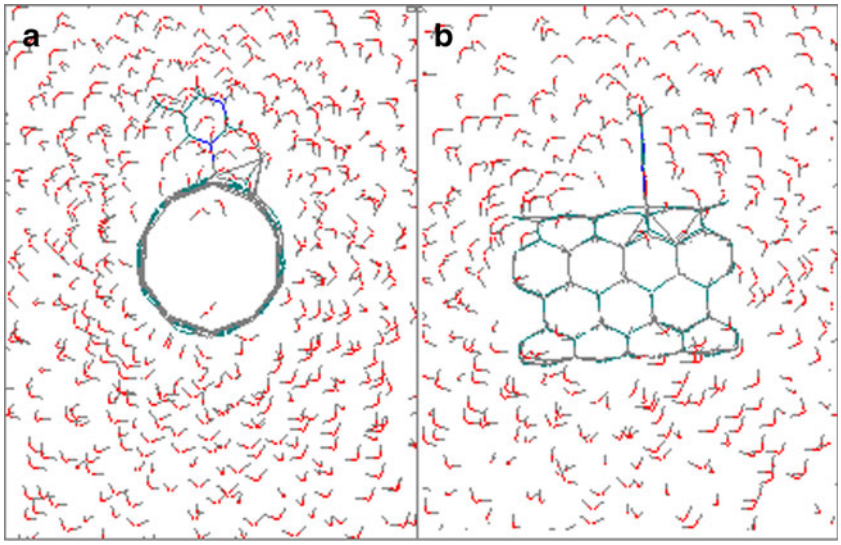

Fig. 4a,b Snapshot of the simulation of SiCNT-Li-T in aqueous solution. **a** Top view, **b** Side view

methods to reproduce experimental results, the real aim is to use these theoretical methods in cases where experiments cannot be performed.

Solvation free energy calculations for each of the solutes (SiCNT-Li and SiCNT-Li-DNA base complexes) were carried out. To model the solvation of SiCNT-Li and its compounds, a simulation was performed on the system with the solute fully represented and its electrostatic and van der Waals parameters decreased to zero. The computed solvation free energies ΔG_{sol} are presented in Table 4. Among all four types of SiCNT-Li-DNA base, in SiCNT-Li- T charges accumulated strongly around Li atom, making the nanotube walls highly reactive to external molecules like H_2O. Thus as expected, the thymine complex of SiCNT-Li had the most negative solvation free energy, and in second place was SiCNT-Li itself, because of the larger electrostatic contribution to the total solvation free energy. The larger charge transfer between thymine and SiCNT makes a higher atomic charge in the nanotube and increases the electrostatic interactions between water molecules and SiCNT and so increases solvation free energies.

Table 5 shows the calculated solvation free energies of adenine, guanine, cytosine and thymine to compute complexation free energies between these DNA bases and SiCNT-Li.

Complexation free energies

Equation 5 was used to calculate each complexation free energy. For this purpose, we need three solvation free energies: solvation free energies of DNA base, SiCNT-Li and, SiCNT-Li- DNA base nanotube. The results are tabulated in Table 5.

It can be seen that the complexation free energy (ΔG_r) of the SiCNT-Li-T species is more negative than that of the other complexes. In fact, of the four DNA bases, only thymine makes a stable compound with SiCNT-Li. As can be seen in Table 5, adenine, guanine and cytosine have positive values of complexation free energies for SiCNT-Li- DNA base complexes. In some embodiments, the extent of functionalization is dependent upon a number of factors, e.g., the reactivity of the CNTs, the reactivity of the functionalizing agent, steric factors, etc.[24]. Therefore, the steric effect of a nucleobase can affect the interaction of DNA bases with SiCNT-Li. In our system, binding strength, which is related to complexation free energy and stability, varies constantly with the DNA base. Thus, thymine has the greatest binding strength with SiCNT-Li due to the formation of a six-membered ring between thymine and SiCNT-Li. As can be seen in Fig. 1, thymine interacts with SiCNT-

Table 3 Summary of Monte Carlo runs. N_{H2O} Number of solvent molecules in the cubic box, *STDEV* standard deviation of the calculated average in the simulation of finite number of steps, <*E*> average energy

Solute	N_{H2O}	<E> (kcal mol^{-1})	STDEV	Relative error
SiC-Li	4009	−140.304	1.6458	0.0117
Adenine	4073	−36.5163	0.1449	0.0040
Guanine	4070	−9.2542	0.0184	0.0020
Cytosine	4071	−9.2460	0.0178	0.0019
Thymine	4069	−9.2130	0.0044	0.0005
SiC-Li-Adenine	4005	−138.0014	0.881642	0.0063886
SiC-Li-Guanine	4004	−136.1444	0.615432	0.0045204
SiC-Li-Cytosine	4004	−139.7772	0.58534	0.0041877
SiC-Li-Thymine	4006	−144.976	0.108782	0.0068664

Table 4 Computed solvation free energies (in kcal mol^{-1})

SPECIES	ΔG_{sol}
SiC-Li	−393.4495
Adenine	−11.6000
Guanine	−21.7000
Cytosine	−20.1000
Thymine	−13.1000
SiC-Li-adenine	−386.7105
SiC-Li-guanine	−389.6550
SiC-Li-cytosine	−395.1725
SiC-Li-thymine	−403.3970

Li via two sites: one from nitrogen to the Si atom of the nanotube (which has a positive charge) and the other through oxygen to Li. These conditions are not suitable for adenine and guanine because of the steric effect of reacting adenine or guanine with SiCNT-L compared with thymine. The steric hindrance of guanine and adenine (two cycle structures) around the SiCNT decreases the stability of their complexes with SiCNT-Li. In the case of cytosine, the existence of the NH_2 group prevents the formation of the six-membered-ring and so the stability of SiCNT-Li-C is less than that of SiCNT-Li-T. Furthermore, greater charge separation in SiCNT-Li-T enhances the stability of this complex in water compared with other DNA base complexes with SiCNT-Li.

The computed intermolecular distance from quantum mechanical calculations indicated that the distance between Li in SiCNT and O in thymine, is 1.75, and that between SiCNT and N in thymine is 1.95. Conversely, in other SiCNTs, the DNA base interacts with Li-doped SiCNT only at one site. In fact, in the thymine complex, we have a six-membered-ring between the DNA base and the NT that stabilizes the complex. Thus, it is expected that SiCNT-Li-T is the most stable complex.

Furthermore, the distance between Li and the DNA base in these complexes are in the following order (Fig. 1):

$$T(1.75\ A\ ) < C(1.86\ A\ ) < A(1.97\ A\ ) < G(2.06\ A\ )$$

Comparison of the distance between Li and the DNA base indicates that thymine must make the most stable complex with SiCNT Li and guanine the least stable. Thus it is predicted that adenine and guanine complexes have less complexation free energy than thymine and cytosine.

Free energy has a relationship with the stability constant of the complex. As can be seen in Table 5, the complex of thymine with SiCNT-Li has the greatest stability constant; therefore, it is the most stable compound. Thus, thymine is a stronger DNA base for reacting with SiCNT-Li.

Table 5 Computed complexation free energies (in kcal mol^{-1}) and stability constants of the complexes

Complex	ΔG_r	log K
SiC-Li-adenine	22.8395	−0.08824
SiC-Li-guanine	11.1815	−0.0432
SiC-Li-cytosine	4.4625	−0.01724
SiC-Li-thymine	−4.1255	0.015939

Radial distribution functions

Radial distribution functions (RDFs) measure the (average) value of a property as a function of an independent variable. A typical example is the radial distribution function $g(r)$, which measures the probability of finding a particle as a function of distance from a "typical" particle relative to that expected from a completely uniform distribution (i.e., an ideal gas with density N/V), considering that by construction, g(r)=1 in ideal gas. Additionally, RDFs are a class of observables properties that characterize the structure of the liquid state. For the NTs, RDF for solvent atom type x, $g_x(r)$ is obtained from the frequency of finding an atom of type x between r and r + dr of the outer surface of the NT (RDF outside the NT) .

Figure 5 depicts the RDF diagrams for the four DNA base Li-doped SiCNTs. These diagrams show water reduced density (ρ_{local}/ρ_{bulk}) around the NTs versus (r) axis, that (r)axis corresponds to the distance from the outside wall of the tube. As can be seen, all the RDF diagrams have two peaks that are in correspondence with the first and second shell-like formations of water around the surface of the NTs. As shown in Fig. 5, the first peak of all NTs occurs at about 2 Å. Comparing among RDFs diagrams, SiCNT-Li-G has the lowest first peak. This is due to the solubility of the NTs. SiCNT-Li-G is the most insoluble sample. Figure 5c,d reveals that the first and second peak for SiCNT-Li- C and SiCNT-Li- T are broader than SiCNT-Li- A and SiCNT-Li- G (Fig. 5a,b). The reason is more solubility of thymine and cytosine complexes, which increase the density of water around the NT. Some water molecules within the shells then point toward each other and cause hydrogen bonding, which provides broad peaks or connected peaks. For all NTs, the second coordination shell can be seen at about 4–5 Å.

As can be seen, the limit of bulk water is also considered. In all cases, the water molecules adopt a bulk structure at distances greater than 8 Å from the NT surface, thus showing the limit of bulk behavior for water. Since the water molecules in this bulk region do not interact with the NT, the differences in density distribution of H_2O molecules between the bulk region

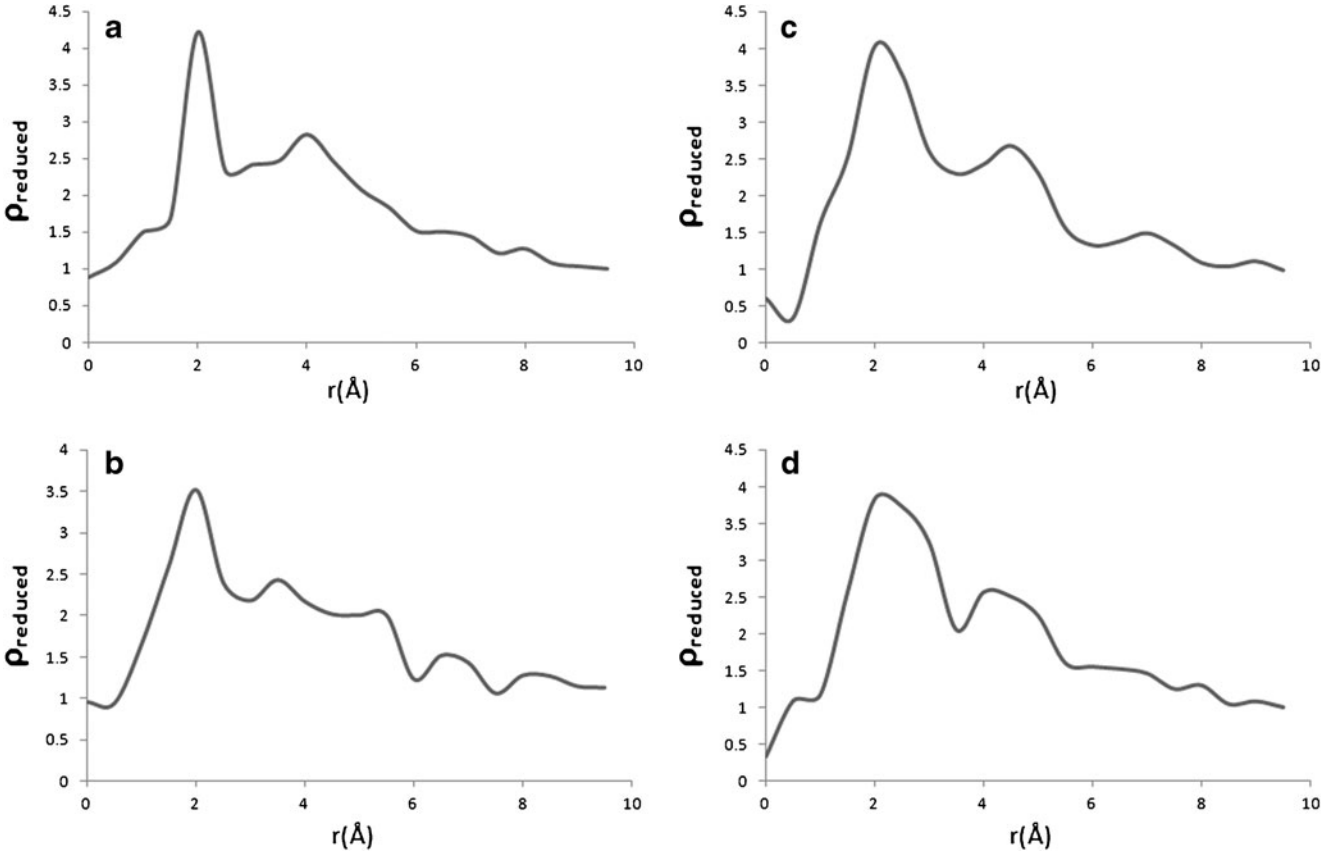

Fig. 5a–d Variation of reduced density of water from the outer surface of SiCNT-Li-DNA base complexes. **a** SiCNT-Li-adenine, **b** SiCNT-Li-guanine, **c** SiCNT-Li-cytosine, **d** SiCNT-Li-thymine

and the interfacial regions are most referred to the adsorption effect of the NT.

Conclusions

As discussed above, fluidic applications of NTs will play an important role in nanotechnology. Considerable efforts have been dedicated to the preparation and functionalization of NTs, and the search for new ideas on water solute samples of NTs. The interaction of biomolecules with single wall NTs is a topic of current research interest. DNA bases have the ability to coordinate a variety of metal ions, and this is a way to interact these biomolecules to NTs and increase their solubility.

In this study, SiCNT-Li and its nucleic acid base complexes were first modeled by quantum machanical calculations and then Monte Carlo simulation was used to calculate solvation free energies plus complexation free energies for the related structures in aqueous solution. These energies are unattainable experimentally because of the lack of volatility of these compounds.

The solvation energies trend for the four DNA bases with SiCNT-Li is as follows: T > C > A > G. The results indicated that the thymine complex of SiCNT-Li has the highest solvation free energy in water and therefore this compound is the most soluble species in water solutions among the four DNA base complexes with SiCNT-Li. Computed complexation free energies for compounds of adenine, guanine, cytosine and thymine with SiCNT-Li indicate that thymine with SiCNT-Li has the lowest complexation free energies, therefore it is the most stable compound in water. This is due to the shorter bond distance between Li and thymine and greater charge density in the complex. Furthermore, the optimized structure of SiCNT-Li- T has a six-membered ring between thymine, Li and NT. This ring structure increases the stability of the thymine complex as compared with the other nucleobases. Therefore, it is concluded that, in the interaction with DNA base, thymine is preferred. Further calculations can be performed to observe whether thymine can increase the solvation of other metal-doped nanotubes as compared with adenine, guanine and cytosine.

References

1. Martin CR, Kohli P (2003) The emerging field of nanotube biotechnology. Nat Rev Drug Discov 2:29–37
2. Lin Y, Taylor S, Li HP, Fernando KAS, Qu LW, Gu LR, Wang W, Zhou B, Sun YP (2004) Advances toward bioapplicationsofcarbon nanotubes. J Mater Chem 14:527–541
3. Bianco A, Kostarelos K, Prato M (2005) Applications of carbonnanotubes in drug delivery. Curr Opin Chem Biol 9(6):674–679
4. Kam NWS, Dai HJ (2005) Carbon Nanotubes as intracellular proteintransporters: generality and biological functionality. J Am Chem Soc 127:6021–6026
5. Kam NWS, O'Connell M, Wisdom JA, Dai HJ (2005) Carbon nanotubes as multifunctional biological transporters and near-infrared agents for selective cancer cell destruction. Proc Natl Acad Sci USA 102(33):11600–11605
6. Wu WWS, Pastorin G, Benincasa M, Klumpp C, Briand JP, Gennaro R, Prato M, Bianco A (2005) Targeted delivery of amphotericinB to cells by using functionalized carbon nanotubes. Angew Chem Int Ed 44(39):6358–6362
7. Kam NWS, Liu ZA, Dai HJ (2006) Carbon nanotubes asintracellular transporters for proteins and DNA: an investigation of theuptake mechanism and pathway. Angew Chem Int Ed 45:577–581
8. Kuzmany H, Kukovecz A, Simon F, Holzweber M, Kramberger C, Pichler T (2004) Functionalization of carbon nanotubes. Synth Met 141(1):113–122
9. Johnston HJ, Hutchison GR, Christensen FM, Peters S, Hankin S, Aschberger K, Stone V (2010) A critical review of the biological mechanisms underlying the in vivo and in vitro toxicity of carbon nanotubes: the contribution of physico-chemical characteristics. Nanotoxicology 4(2):207–246
10. Lam CW, James JT, McCluskey R, Arepalli S, Hunter RL (2006) A review of carbon nanotube toxicity and assessment of potential occupational and environmental health risks. Crit Rev Toxicol 36 (3):189–217
11. Murr LE, Garza KM, Soto KF, Carrasco A, Powell TG, Ramirez DA, Guerrero PA, Lopez DA, Venzor J (2005) Cytotoxicity assessment of some carbon nanotubes and related carbon nanoparticle aggregates and the implications for anthropogenic carbon nanotube aggregates in the environment. Int J Environ Res Public Health 2(1):31–42
12. Park EJ, Roh J, Kim SN, Kang MS, Lee BS, Kim Y, Choi S (2011) Biological toxicity and inflammatory response of semi-single-walled carbon nanotubes. PLoS One 6(10):e25892
13. Mwangi JN, Wang N, Ritts A, Kunz JL, Ingersoll CG, Li H, Deng B (2011) Toxicity of silicon carbide nanowires to sediment-dwelling invertebrates in water or sediment exposures. Environ Toxicol Chem 30(4):981–987
14. Zhang YF, Huang HC (2008) Comput Mater Sci 43:664–669
15. Mpournpakis G, Froudakis GE, Lithoxoos GP, Samios J (2006) Nano Lett 6:1581–1583
16. Zhao MW, Xia YY, Li F, Zhang RQ, Lee ST (2005) Phys Rev B 71:085312-1-7
17. Cicero G, Galli G (2004) J Phys Chem B 108:16518–16524
18. Haeri HH, Ketabi S, Hashemianzadeh SM (2012) J Mol Model 18:3379–3388
19. Mavrandonakis A, Froudakis GE, Schnell M, Muhlhäuser M (2003) From pure carbon to silicon-carbon nanotubes: an ab-initio study. Nano Lett 3:1481–1484
20. Sun XH, Li CP, Wong WK, Wong NB, Lee CS, Lee ST, Teo BK (2002) Formation of silicon carbide nanotubes and nanowires via reaction of silicon (from disproportionation of silicon monoxide) with carbon nanotubes. J Am Chem Soc 124:14464–14471
21. Zhao MW, Xia YY, Li F, Zhang RQ, Lee S-T (2005) Strain energy and electronic structures of silicon carbide nanotubes: density functional calculations. Phys Rev B 71:085312.1–085312.6
22. Miyamoto Y, Yu BD (2002) Computational designing of graphitic silicon carbide and its tubular forms. Appl Phys Lett 80:586–588
23. Menon M, Richter E, Mavrandonakis A, Froudakis G, Andriotis AN (2004) Structure and stability of SiC nanotubes. Phys Rev B 69:115322.1–115322.4
24. Menon M, Richter E, Mavrandonakis A, Froudakis G, Andriotis AN (2004) Phys Rev B69:115322–115334
25. Mananghaya M, Rodulfo E, Santos GS, Villagracia A (2012) Theoretical investigation on the solubilizationin water of functionalized single-wall carbon nanotubes. J Nanotechnol 2012:1–6
26. Star A, Liu Y, Grant K, Ridvan L, Stoddart JF, Steuerman DW, Diehl MR, Boukai A, Heath JR (2003) Noncovalent side-wallfunctionalization of single-walled carbon nanotubes. Macromolecules 36(3):553–560
27. Chen RJ, Zhang Y, Wang D, Dai HJ (2001) Noncovalentsidewall-functionalization of single-walled carbon nanotubes for protein immobilization. J Am Chem Soc 123(16):3838–3839
28. Dyke CA, Tour JM (2004) Covalent functionalization of single-walled carbon nanotubes for materials applications. J Phys Chem A 108(51):11151–11159
29. Prato M, Bianco A (2003) Can carbon nanotubes be considered useful tools for biological applications. Adv Mater 15(20):1765–1768
30. Huang W, Taylor S, Fu K, Lin Y, Zhang D, Hanks TW, Rao AM, Sun YP (2002) Attaching proteins to carbon nanotubes via diimi-deactivatedamidation. Nano Lett 4:311–314
31. Lin Y, Allard LF, Sun YP (2004) Protein-affinity of singlewalled-carbon nanotubes in water. J Phys Chem B 108(12):3760–3764
32. Bianco A, Kostarelos K, Partidos CD, Prato M (2005) Chem Commun 5:571–577
33. Lacerda L, Bianco A, Prato M, Kostarelos K (2008) J Mater Chem 18:17–22
34. Lu F, Gu L, Meziani MJ, Wang X, Luo PG, Veca LM, Cao L, Sun YP (2009) Adv Mater 21:139–152
35. Gowtham S, Scheicher RH, Pandey R, Karna SP, Ahuja R (2008) Nanotechnology 19:125701-1-6
36. Zheng M, Jagota A, Semke ED, Diner BA, Mclean RS, Lustig SR, Richardson RE, Tassi NG (2003) Nat Mater 2:338–342
37. Wang Y (2008) J Phys Chem C 112:14297–14305
38. Varghese N, Mogera U, Govindaraj A, Das A, Maiti PK, Sood AK, Rao CNR (2009) ChemPhysChem 10:206–210
39. Zhao C, Peng Y, Song Y, Ren J, Qu X (2008) Small 4:656–661
40. Gao X, Xing G, Yang Y, Shi X, Liu R, Chu W, Jing L, Zhao F, Ye C, Yuan H, Fang X, Wang C, Zhao Y (2008) J Am Chem Soc 130:9190–9191
41. Umadevi D, Sastry GN (2011) Quantum mechanical study of physisorption of nucleobaseson carbon materials: graphene versus carbon nanotubes. J Phys Chem Lett 2:1572–1576
42. Zhong X, Slough WJ, Pandey R, Friedrich C (2012) Interaction of nucleobases with silicon nanowires: a first-principles study. Chem Phys Lett 553:55–58
43. Kharisov BI, Kharissova OV, Gutierrez HL, Méndez UO (2009) Ind Eng Chem Res 48:572–590
44. Gu Z, Liang F, Chen Z, Sadana A, Kittrell C, Billups WE, Hauge RH, Smalley RE (2005) In situ Raman studies on lithiated single-wall carbon nanotubes in liquid ammonia. Chem Phys Lett 410 (4):467–470
45. Hashemianzadeh SM, FarajiSh, Amin A, Ketabi S (2008) Theoretical study of the interactions between isolated DNA bases and various groups IA and IIA metal ions by ab initio calculations. Monatshefte fur chemie, chemical monthly 139: 89–100
46. Leach AR (1996) Molecular modeling—principles and application. Longman, Essex

47. Redmill PS, Capps SL, Cummings PT, McCabe C (2009) A molecular dynamics study of the Gibbs free energy of solvation of fullerene particles in octanol and water. Carbon 47:2865–2874
48. Jorgensen WL, Chandrasekhar J, Madura JD, Impey RW, Klein ML (1983) Comparison of simple potential functions for simulating liquid water. J Chem Phys 79:926–935
49. Jorgensen WL (1981) Transferable intermolecular potential functions for water, alcohols, and ethers. Application to liquid water. J Am Chem Soc 103:335–340
50. Jia Y, Wang M, Wu L (2007) Sep Sci Technol 42:3681–3695
51. Lithoxoos GP, Samios J (2008) J Phys Chem C 112:16725–16728
52. Aaqvist J (1990) Ion-water interaction potentials derived from free energy perturbation simulations. J Phys Chem 94(21):8021–8024
53. Pranata J, Wierschke SG, Jorgensen WL (1991) J Am Chem Soc 113:2810–2819
54. Hansen JP, McDonald IR (1991) Theory of simple liquids. Academic, London
55. Beveridge DL, Capua D, Annu FM (1989) Rev Biophys Biophys Chem 18:431
56. Monajjemi M, Ketabi S, Hashemian Zadeh M, Amiri A (2006) Biochem Mosc 71(1):S1–S8
57. Lippert B (2000) Coord Chem Rev 200–202:487–516
58. Petersson GA, Al-Laham MA (1991) A complete basis set model chemistry. II. Open-shell systems and the total energies of the first-row atoms. J Chem Phys 94:6081–6090
59. Schmidt MW, Baldridge KK, Boatz JA, Elbert ST, Gordon MS, Jensen JH, Koseki S, Matsunaga N, Nguyen KA, Su SJ, Windus TL, Dupuis M, Montgomery JA (1993) J Comput Chem 14:1347–1363
60. Metropolis N, Rosenbulth AW, Rosenbulth MN, Teller AH, Teller E (1953) Equation of state calculations by fast computing machines. J Chem Phys 21:1087–1093
61. Wang Y (2008) Theoretical evidence for the stronger ability of thymine to disperse SWCNT than cytosine and adenine: self-stacking of DNA bases vs their cross-stacking with SWCNT. J Phys Chem C 112:14297–14305
62. Zheng M, Jagota A, Semke ED, Diner BA, Mclean RS, Lustig SR, Richardson RE, Tassi NG (2003) DNA-assisted dispersion and separation of carbon nanotubes. Nat Mater 2(5):338–342
63. Das A, Sood AK, Maiti PK, Das M, Varadarajan R, Rao CNR (2008) Chem Phys Lett 453:266–273
64. Gowtham S, Scheicher RH, Ahuja R, Pandey R, Karna SP (2007) Phys Rev B 76:033401-1-4
65. Antony J, Grimme S (2008) Phys Chem Chem Phys 10:2722–2729
66. Kollman PA (1993) Chem Rev 93:2395–2417